

## Electronic Supplementary Information

### **Competing Ferro- and Antiferromagnetic Interactions in a Hexagonal Bipyramidal Nickel Thiolate Cluster**

Tomohiko Hamaguchi,<sup>a</sup> Michael D. Doud,<sup>b</sup> Jeremy Hilgar,<sup>b</sup> Jeffrey D.

Rinehart,<sup>b</sup> and Clifford P. Kubiak<sup>\*,b</sup>

<sup>a</sup> *Department of Chemistry, Faculty of Science, Fukuoka University, 8-19-1  
Nanakuma, Jonan-ku, Fukuoka 814-0180, Japan*

<sup>b</sup> *Department of Chemistry and Biochemistry, University of California – San  
Diego, 9500 Gilman Drive, Mail Code 0358, La Jolla, CA 92093-0358, USA*

**Instrumentation.**

Powder X-ray diffraction (PXRD) data were recorded on a Bruker D8 Advance equipped with a 1-D Lynxeye silicon strip detector and Cu radiation ( $1.54178 \text{ \AA}$ ). The C, H, N and S analysis was performed by NuMega Resonance Labs. Magnetic measurements were carried out on a Quantum Design MPMS3.

**X-ray crystallography.**

X-ray diffraction data were collected using a Bruker APEX-II CCD diffractometer, with Mo  $K\alpha$  radiation ( $\lambda = 0.71070 \text{ \AA}$ ). Multi-scan absorption corrections were applied to the intensity data. The structure was solved using the direct method (using *SHELXS-2013/4*)<sup>1</sup> and refined using the full-matrix least-squares method using  $F^2$  (*SHELXL-2013/4*)<sup>1</sup> operated by *Olex2* software package<sup>2</sup> and *Yadokari-XG* software package.<sup>3</sup> All non-hydrogen atoms were refined using anisotropic parameters. Hydrogen atoms were included in the calculated positions and refined using a riding model. Crystallographic diagrams were obtained using the ORTEP program.<sup>4</sup> Crystal data are shown in

Table S1.

### **Magnetometry.**

The magnetic sample was prepared by adding fine crystalline powder to a VSM powder sample holder from Quantum Design. The addition was carried out in small increments and after each increment the sample in the holder was firmly pressed into a pellet. This was done so as to reduce any crystallite orientation during the measurements. All magnetic measurements were performed on a Quantum Design MPMS-3 SQUID Magnetometer with a four second scan speed. The compound's magnetic susceptibility was measured from 2 to 300 K using an applied field of 1000 Oe. The variable-temperature magnetization measurements were carried out at 2.00 K, 4.00 K, and 6.00 K from 0 to 70000 Oe applied field. All data were corrected for diamagnetic contributions using Pascal's constants ( $\chi_D = -0.00139136$  emu/mol).

The best fit of the  $\chi_M T$  data was obtained using the program *PHI*.<sup>5</sup> Isotropic exchange interactions between adjacent spin centers were considered and a total of

two exchange parameters were defined. The parameter  $J_{\text{FM}}$  represented planar-planar Ni coupling and  $J_{\text{AFM}}$  was defined for planar-capping coupling. The following parameters of best fit were found:  $J_{\text{FM}} = 12.9 \text{ cm}^{-1}$ ,  $J_{\text{AFM}} = -30.7 \text{ cm}^{-1}$ ,  $g = 2.1$  ( $R = \Sigma (\chi_{\text{M}} T_{\text{Obs}} - \chi_{\text{M}} T_{\text{Calc}})^2 / \Sigma \chi_{\text{M}} T_{\text{Obs}}^2 = 7.26 \times 10^{-5}$ ).

The best fit of the variable temperature magnetization data was obtained using MagProp, a sub-routine of the Data Analysis and Visualization Environment.<sup>6</sup> This data was modelled as an  $S = 4$  giant spin using a Hamiltonian containing an average axial zero-field splitting term and a Zeeman term (Eq. 2). The following parameters of best fit were found:  $|D| = 0.35 \text{ cm}^{-1}$ ,  $g = 2.2$  ( $R = \Sigma (M_{\text{Obs}} - M_{\text{Calc}})^2 / \Sigma M_{\text{Obs}}^2 = 1.11 \times 10^{-4}$ ).

## Synthesis.

A  $\text{CH}_2\text{Cl}_2$  solution (15 ml) of 2-pySH (1.639 g, 14.74 mmol) was added to a  $\text{CH}_3\text{CN}$  (15 ml) solution of  $[\text{Ni}(\text{H}_2\text{O})_6](\text{BF}_4)_2$  (509.2 mg, 1.496 mmol), and the mixture was stirred overnight. The resulted dark green-yellow solution was evacuated to dryness. The residual solid was dissolved to  $\text{CH}_2\text{Cl}_2$  and was filtrated to

remove insoluble material. The filtrate was evacuated to dryness. The residual solid was dissolved to small amount of  $\text{CH}_2\text{Cl}_2$  and excess amount of 2-propanol was added to the solution. The resulted precipitate was collected by filtration. The obtained crude product was purified by recrystallization. A  $\text{CH}_3\text{CN}$  solution of the crude product and excess  $\text{NH}_4\text{PF}_6$  was placed under 2-propanol vapor for seven days, and the resulted deep brown cubic crystals were collected by filtration. The crystals were washed with water, 2-propanol and diethyl ether and were dried *in vacuo*. Yield 171.3 mg (35.0 %). Anal. found: C, 33.28; H, 2.94; N, 9.38; S, 14.73 %; calcd. for  $\text{C}_{72}\text{H}_{66}\text{F}_{24}\text{N}_{18}\text{Ni}_8\text{P}_4\text{S}_{12}$ : C, 33.03; H, 2.54; N, 9.63; S, 14.70 %. UV-vis ( $\text{CH}_3\text{CN}$ )  $\lambda_{\text{max}}$ , nm ( $\epsilon$ ,  $\text{dm}^3 \text{ mol}^{-1} \text{ cm}^{-1}$ ) 225sh (93700), 270sh (66500), 320 (63400).

Table S1 Crystal Data

Formula	C <sub>72</sub> H <sub>66</sub> N <sub>18</sub> Ni <sub>8</sub> S <sub>12</sub> P <sub>4</sub> F <sub>24</sub>
Formula Weight	2617.6
Crystal System	monoclinic
Space group	<i>P</i> 2 <sub>1</sub> / <i>n</i> (No. 14)
<i>a</i> /Å	13.9583(3)
<i>b</i> /Å	22.5215(5)
<i>c</i> /Å	15.3686(4)
$\alpha$ /°	90
$\beta$ /°	92.3771(13)
$\gamma$ /°	90
<i>V</i> /Å <sup>3</sup>	4827.1(2)
<i>Z</i>	2
<i>D</i> <sub>calc</sub> /g•cm <sup>-3</sup>	1.801
$\mu$ (MoK $\alpha$ )/mm <sup>-1</sup>	1.949
F(000)	2632
Crystal Size/mm <sup>3</sup>	0.05 × 0.05 × 0.10
Data Collection	
Temperature/K	100
Radiation [Angstrom]	Mo K $\alpha$ , 0.71073
Theta Min, Max/°	1.7, 25.3
Dataset	-16: 15 ; -26: 27 ; -15: 18
Tot., Uniq. Data, <i>R</i> (int)	39258, 8804, 0.021
Observed Data [ <i>I</i> > 0.0 sigma( <i>I</i> )]	7789
Refinement	
<i>N</i> <sub>ref</sub> , <i>N</i> <sub>par</sub>	8804, 625
<i>R</i> , w <i>R</i> <sub>2</sub> , <i>S</i>	0.0366, 0.1040, 1.05
Max. and Av. Shift/Error	0.00, 0.00
Min. and Max. Resd. Dens./e•Å <sup>-3</sup>	-0.86, 0.83

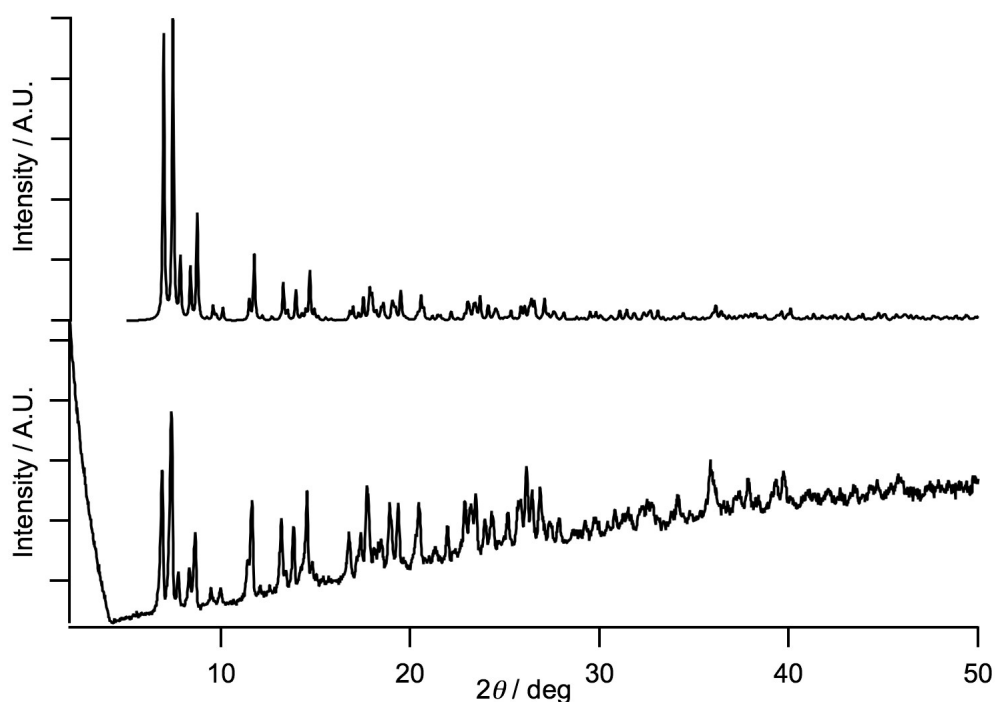


Figure S1. X-ray powder diffraction pattern of complex **1** (top: simulated pattern,  
bottom : observed data)

#### Reference

1. G. M. Sheldrick, *Acta Crystallographica Section A*, 2008, **64**, 112-122.
2. O. V. Dolomanov, L. J. Bourhis, R. J. Gildea, J. A. K. Howard and H. Puschmann, *J. Appl. Crystallogr.*, 2009, **42**, 339-341.
3. C. Kabuto, S. Akine, T. Nemoto and E. Kwon, *J. Cryst. Soc. Jpn.*, 2009, **51**, 218-224.
4. L. Farrugia, *J. Appl. Crystallogr.*, 2012, **45**, 849-854.
5. N. F. Chilton, R. P. Anderson, L. D. Turner, A. Soncini and K. S. Murray, *J. Comput. Chem.*, 2013, **34**, 1164-1175.
6. R. T. Azuah, L. R. Kneller, Y. Qiu, P. L. W. Tregenna-Piggott, C. M. Brown, J. R. D. Copley and R. M. Dimeo, *J. Res. Natl. Inst. Stan. Technol.*, 2009, **114**, 341-358.